CFD Letters

Journal homepage:
https://semarakilmu.com.my/journals/index.php/CFD_Letters/index
ISSN: 2180-1363

Studying How the Size of Energy Storage Tanks with Sodium Nitrate Affects Their Performance

Ameer Abid Muslim[1], Ayad Ali Mohammed[2,*], Nadwan majeed ali[1]

[1] Al-Furat Al-Awsat Technical University, Al- Mussaib Technical Institute, 51009, Iraq
[2] Al-Furat Al-Awsat Technical University, Al-Mussaib Technical College, Babylon 51006, Iraq

ARTICLE INFO

Article history:
Received 4 February 2024
Received in revised form 8 March 2024
Accepted 5 April 2024
Available online 30 September 2024

Keywords:
Phase change Material; Grashof number; tank dimensions; Ansys Fluent; alumina

ABSTRACT

Energy storage helps to balance the difference between how much energy is made and how much is used. It also makes energy systems work better and be more reliable. This is why energy storage is so important. This technology saves money by collecting and using energy that would have been wasted. Storing heat using materials that change from one phase to another is a well-respected way to store thermal energy. Exploring how to store energy in tanks with special material that changes from one phase to another is a new and interesting topic in the energy field. Sodium nitrate is the material used in this study. This talk is about how the amount of alumina and the size of the tank affect how molten sodium nitrate acts for a period of time. This study looks at how the size of a shape compared to its length affects the Grashof number. As a result, ten different sizes of the tank are considered. This study looks at what happens when we use a special material in energy storage tanks. We used a computer program called Ansys Fluent to analyze the results. To reach this goal, first we need to compare the sizes we need with the Gershoff numbers we measured for different widths. Increasing the amount of alumina in sodium nitrate makes the temperature inside the tank more even. Adding alumina particles to sodium nitrate has less of a effect when the tank is shorter and wider. As the tank goes from state 1 to state 7, where the width and height are the same, the temperature change graphs become less curvy. This drop means the phase-change material is melting slower. The temperature changes in the tank depend on how big the tank is. If the tank is bigger, the temperature changes more slowly. Adding more alumina to sodium nitrate does not make a big difference in how heat is spread out in tanks that are wider than they are tall.

1. Introduction

Phase change materials (PCM) are a new class of thermal substances that change their physical state to store absorbed energy as latent energy. The Earth is seeing a rapid temperature increase due to the widespread growth of industry and metropolitan areas and the continuous escalation of greenhouse gas emissions. Global warming causes ice melting in the Arctic and Antarctic areas,

* *Corresponding author.*
E-mail address: ayadia1@atu.edu.iq (Ayad Ali Mohammed)

https://doi.org/10.37934/cfdl.17.2.4359

leading to environmental disasters. Nevertheless, economists argue that the unwavering pursuit of economic progress requires the ongoing enlargement of industry and metropolitan regions. Therefore, in recent years, researchers have been investigating several techniques to store thermal waste energy in suitable forms for future utilization. Energy storage helps reduce the gap between energy supply and demand while improving the efficiency and reliability of energy-producing systems. It plays a vital role in the field of energy storage. This technique minimizes costs by harnessing and using surplus energy. Thermal energy storage systems can help power plants work better by using less energy and becoming more efficient. This can also reduce the need for storage and lower costs. Using materials that change from one phase to another to store thermal energy has become a popular and fascinating technique in the last few decades. Phase-change materials can store energy by absorbing or releasing heat that is not noticeable. Heat moves when a solid turns into a liquid, or when a liquid turns into a solid. A phase transition is when the circumstances change. Phase transition materials have a set temperature where they take in and let out heat. Making energy storage better and finding the best size for the tank is a big deal when designing energy storage tanks [1].

Thermal energy storage (TES) is achieved using sensible heat and latent heat technologies. This is because the latent technique can retain energy at a consistent temperature and exhibits a greater density than the sensible approach [2]. Utilizing the latent heat technique is often more efficient and feasible than other accessible alternatives. This approach uses phase change materials (PCM) with a high latent heat capacity to store substantial quantities of heat effectively. Furthermore, they have disadvantages, such as limited heat conductivity and heightened viscosity. Hence, encountering imperfections, such as insufficient heat conductivity and non-viscous fluid, is inevitable. In order to tackle the issue of inadequate thermal conductivity, many strategies have been utilized, such as the incorporation of fins [3], porous media [4], magnetic fields [5], and nanoparticles [6], employing techniques including encapsulation and adhesion. Encapsulated micro or nanophase change materials (PCM) have several applications, such as energy storage, namely for renewable and alternative energies [7], and enhancing thermal comfort in buildings [8]. Thermal comfort may be achieved, and energy can be saved using phase-change materials with a suitable temperature range for the fusion process. It is released by freezing if required [9].

Ames and Kamel [8] conducted research to gain a deeper comprehension of the process of water solidification within spherical capsules employed in heat storage devices. Semi-empirical formulas can be used to predict the ice mass of a sphere at any given position. The storage system utilizes dimensionless Fourier and Stefan numbers. The researchers found that, during 70% of the discharge duration, a substantial quantity of the cold energy could be recovered from the capsules. Brahim and Ahn [10] conducted a computer analysis of the solidification process in a two-dimensional axisymmetric system confined by two concentric cylinders. The authors employed the finite difference approach to solve the governing equations. In order to assess the efficacy of varying numbers of nodes, as well as explicit and implicit approaches, the researchers conducted tests. Upon comparison with the implicit technique, the researchers observed that the explicit system yielded more consistent results. Ramachandran *et al.,* [11] did a quantitative study on the solidification process occurring within a rectangular cage. The enclosure had thermally insulated bottom and upper walls, while the lateral surfaces were kept at a constant temperature. The alternate direction implicit finite difference approach was employed to solve the governing equations once they were transformed into dimensionless form. Shih and Chou [12] employed an analytical iteration method to elucidate the process of solidification, both internally and externally, of a fully saturated liquid within spherical containers. The analytical iteration technique is used to simplify the diffusion equation. The study conducted by Velraj *et al.,* [13] examined the

solidification process of a phase change material (PCM) in a vertical tube using a combination of computational and experimental methods. A study was conducted to examine the effects of incorporating fins to improve heat conduction. The authors employed an implicit finite difference methodology to solve the governing equations. The enthalpy technique was employed to characterize the solid-liquid interface. In the absence of a fin, the heat flow at the inner surface of the tube experienced a significant reduction and maintained a consistently low level during the whole operation.

Thermal energy storage (TES) experiments were conducted by Lino *et al.,* [14] on a flat solar collector utilizing paraffin wax as a phase change material (PCM) and an additional PCM containing 1.0% weight of copper nanoparticles. The researchers expanded upon previous studies involving the incorporation of phase transition elements into nanoparticles, with the aim of enhancing the performance of solar collectors. There is a research report written by Zhai and their colleagues [15], which was published in 2017. The study investigated the efficacy of incorporating nanoparticles and high-performance evacuated tube collector (HPETC) technology into an evacuated tube solar collector equipped with a heat pipe, with the addition of a phase change material (PCM). The study employed both empirical and computational analysis. The addition of three weight percent of expanded graphite successfully raised the energy storage efficiency of PCM to 40.17%.2018 marks the current year. Lee and his colleagues. The modifications performed in Ref. [16] were limited to replacing the heat pipe with copper water as the heat transfer medium in the NEPCM. The energy storage efficiency of this groundbreaking device was 39.98%. The charging mechanism of a flat plate solar collector was statistically investigated by multiple authors [14]. The storage unit, or NEPCM, consists of vertically arranged slabs containing phase change materials that are reinforced with nanoparticles [15]. The researchers utilized CeO2-Parafins, a nano-reinforced phase change material (PCM), within a thermosiphon evacuated tube solar collector (ETSC) to evaluate its heat storage capacities. The optimal composition for the NEPCM consists of CeO2 nanoparticles, which constitute 1% of the overall composition. The study conducted by a study [16] investigated the turbulent flow of single and hybrid nanofluids in a conical diffuser. The study investigates the impact of varying Reynolds numbers and volume fractions of nanoparticles on pressure losses and heat transfer coefficients. The diffuser contains Al2O3, NEPCM Al2O3 nanofluids, and NEPCM nano-encapsulated phase change materials.

Latent Heat Thermal Energy Storage (LHTES) systems are an innovative advancement with practical applications, as evidenced by the research conducted by Hussein Togun and colleagues [17]. The authors propose a refined and readily applicable approach for efficiently storing and releasing thermal energy. Bhim Kumar Choure and colleagues [18] have found that the performance of phase transition materials can be enhanced by a combination of innovative and conventional methods. The Latent Heat Thermal Energy Storage (LHTES) system has been developed as a reliable option for storing and releasing thermal energy on demand. Various fin configurations with distinct shapes and orientations have been employed to investigate the augmentation of heat transmission. Furthermore, researchers have examined the effect of altering the form on the speed of heat transfer. Scientists have investigated the arrangement of various melting points of Phase Change Materials (PCMs) and the duration required for their charging and discharging processes. An investigation was conducted to analyze the effects of varying weight percentages of metal oxide, carbon fiber, carbon nanotube, graphene, and nanoparticles. Graphene's exceptional thermal conductivity renders it an outstanding medium for heat transport. The hybrid TES prototype, as delineated by Lukas Kasper and colleagues [19], is characterized by the application of meticulous modeling and empirical measurement results. By conducting parameter optimization, the uncertain parameters of the model are determined, resulting in

numerical models that yield satisfactory validation outcomes. The PCM containers, which have been adapted for the laboratory-scale RSS, has the capacity to accommodate an additional thirty percent of thermal energy. The objective of the study conducted by Giulia Righetti *et al.,* [20] was to showcase the practical performance of a novel 18 kWh latent thermal energy storage system. This system efficiently stores and releases cold energy by utilizing the solid/liquid phase change process of 300 kg of a biobased phase change material with a melting point of 9 °C. The technique utilizes roll-bond technology.

This research looks at a tall aluminum tank that has a material inside that can change from solid to liquid, along with air. The PCM used is sodium nitrate, which melts at 306°C. We use computer models to simulate how the liquid in the tank melts and solidifies. The outside part of the tank wall is always at the same temperature. The simulation shows how heat can move through conduction and natural convection. Research is looking at how adding aluminum to sodium nitrate is affecting things. Most of the sodium nitrate and the amount of liquid in the tank stayed almost the same during the experiment. Changing the height and diameter of the tank can change its shape. This is done by changing the ratio of the tank's height and diameter, or the proportions of its inside measurements. This makes the cylinder be able to be different shapes, like short and strong or long and thin. Skinny, short cylinders have a big circumference and are small in size. The way the tank is designed affects how sodium nitrate melts and freezes because the amount of the substance stays about the same. This study wants to find out how the shape of a container and the amount of alumina in it affect how sodium nitrate melts and solidifies.This article specifically examines simultaneously the effect of adding alumina to sodium nitrate and the dimensions of the tank, which has not been observed in previous studies.

2. Governing Equations and Boundary Conditions

We are examining a vertical cylinder in the presence of a gravitational field, as shown in Figure 1. The issue exhibits axisymmetry concerning the vertical axis of the cylinder. The radial axis corresponds to the y-axis, while the vertical axis corresponds to the x-axis. The vertical cylinder holds salt and air as the phase change material (PCM). The salt utilized for this investigation is sodium nitrate. The gravitational force vector is directed opposite to the positive x-axis. There are ten states under consideration. A tank with height H, diameter D and thickness t is considered. The height of salt in this tank is hs and the rest is air. All states under consideration have a uniform wall thickness of 0.5mm. Initially, the system's temperature is low enough for sodium nitrate to exist in its solid state. The temperature at the beginning is 576.95 Kelvin. The exterior wall of the cylinder experiences a sudden and significant shift in temperature, which is represented in the model as an isothermal boundary condition. The designated temperature is 10 Kelvin higher than the melting point of sodium nitrate. Conduction is the method by which heat is transferred within the solid wall. Heat transport between Sodium Nitrate and air occurs via conduction and natural convection. Alpha-phase alumina is the strongest and most complex oxide ceramic. Its high hardness, excellent dielectric properties, shock resistance, and good thermal properties make it the material of choice for various applications. Alumina with high purity shows good oxidation resistance up to 1925 degrees Celsius. It has high chemical resistance against all gases except wet fluorine and is also resistant to all acidic substances except hydrofluoric and phosphoric acids. Chemical reactions usually occur at high temperatures, in the presence of alkaline vapors, especially at low purity. In this project, one of the research objectives is to investigate the effect of adding alumina to sodium nitrate.

The simulation utilized the subsequent material attributes and input parameters according to Table 1.

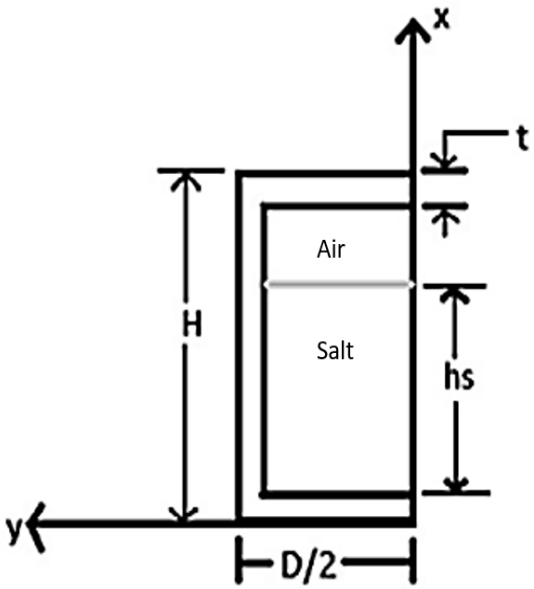

Fig. 1. Cylinder schematic

Table 1
Simulation utilized the subsequent material attributes and input parameters [21]

characteristic	the amount of
The mushy zone temperature dependent density function of Sodium Nitrate	66282.45 – 111T
The liquid phase temperature dependent density function of Sodium Nitrate	2628.5 – 1.2424T
The temperature dependent dynamic viscosity function of Sodium Nitrate	0.011916 - 0.00001533T
The latent heat of fusion of Sodium Nitrate	178000 J/kg
The melting temperature of Sodium Nitrate	579.95 K
The temperature dependent specific heat function of Sodium Nitrate	444.53 – 2.18T
The temperature dependent thermal conductivity of Sodium Nitrate	0.305762 + 0.000447T
The specific heat of Aluminum	871 J/kg-K
thermal conductivity of Aluminum	202.4 W/m-K
Alumina density	3.72g/cc

The equations governing the transfer of momentum and energy in unrestricted motion are derived from the fundamental conservation laws. The significance of inertia and viscosity forces remains, along with energy transmission through displacement and diffusion. The equations that govern this model, as referenced by Ref. [22], may be expressed in the following manner:

The equation for the conservation of mass:

$$\frac{\partial \rho}{\partial t} + \frac{\partial(\rho u)}{\partial x} + \frac{\delta(\rho v)}{\delta y} = 0 \tag{1}$$

Navier-Stokes equation in the x direction [23]:

$$\frac{\partial u}{\partial \mathrm{t}} + u\frac{\partial u}{\partial x} + v\frac{\delta v}{\delta y} = v\left(\frac{\partial^2 u}{\partial x^2} + \frac{\partial^2 u}{\partial y^2}\right) - \beta g(T - T_0) \tag{2}$$

Energy equation [24]:

$$\frac{\partial T}{\partial \mathrm{t}} + u\frac{\partial T}{\partial x} + v\frac{\delta T}{\delta y} = v\left(\frac{\partial^2 T}{\partial x^2} + \frac{\partial^2 T}{\partial y^2}\right) \tag{3}$$

2.1 Governing Equations for PCM Housing

The governing equations for transient analysis of phase change material melting comprise the Navier-Stokes momentum, continuity, and energy equations. The Boucinsk approximation is employed to simulate the buoyancy forces. Below are the equations:

$$\nabla.\vec{v} = 0 \tag{4}$$

Momentum equation [25]:

$$\rho\frac{\partial \vec{v}}{\partial t} + \rho(\vec{v}.\nabla)\vec{v} = -\nabla P + \mu\nabla^2\vec{v} + \rho\vec{g}\beta(T - T_O) \tag{5}$$

Energy equation:

$$\rho_S C_{ps}\left(\frac{\partial T_S}{\partial t} + \vec{v}.\nabla T\right) = \nabla(k_S\nabla T) \tag{6}$$

The subscript "s" denotes the presence of solid or enclosed phase change material (PCM). The energy equation governing the solid-liquid interface during the melting process may be represented as:

$$k_S\frac{\partial T_S}{\partial n}\bigg|_S - k_l\frac{\partial T_S}{\partial n}\bigg|_S = \rho_S L\frac{dS_N}{dt} \tag{7}$$

S represents the interface where a phase shift occurs between a solid and a liquid. The vector n represents the perpendicular direction to the boundary between the solid and liquid phases, whereas L denotes the heat required for a substance to undergo fusion. During the freezing process, the subscripts l and s are swapped, and the latent heat of fusion is involved. The equation replaces the variable L with its negative counterpart (-L).

Gershoff's number is calculated as follows [26]:

$$Gr = \frac{g\beta(T_s - T_b)D^3}{\nu^2} \tag{8}$$

3. Results

This section presents the findings from examining energy storage tanks incorporating phase change material utilizing the AnsysFluent program. To achieve this objective, the initial step involves presenting the ratio between the required dimensions and the Gershoff numbers acquired for various diameters. Next, we examine the convergence process of the mesh and the solution's independence from the grid. Subsequently, the study will show state the outlines of the liquid portion and the corresponding temperature, culminating in a comprehensive discussion of the findings through a diagram.

3.1 Aspect Ratio and Groshoff Number

The dimensions ratio and Gershoff numbers derived from the analysis are displayed in Table 2.

Table 2
Tank dimensions and calculated Gershoff numbers

state of	diameter (mm)	height(mm)	Gershoff's number
1	20	200	213389
2	21.5	173	265093
3	23.7	142.5	355081
4	25.2	126	426859
5	27	109.7	525018
6	34	69.2	1048384
7	43.1	43.1	2135577
8	47	36.2	2769345
9	55	26.05	4437840
10	70	16.35	9149085

3.2 The Independence of the Solution from the Network

The analysis focuses on a rectangular piece of the tank's plate for the present study. Therefore, the most suitable components for discretization are quadrilateral elements, as shown in Figure 2. These pieces align with the research's geometry and provide the closest approximation. However, we must address the crucial inquiry of determining the optimal size for these components. To achieve this objective, the dimensions of the elements for state three were modified based on the values provided in Table 2. We set the temperature boundary conditions for the three left, right, and upper walls to 610 K and for the lower wall to 597/5. The average temperature inside the tank was then measured, and the results were analyzed to determine the solution's independence from the network. Figure 3 presents the findings.

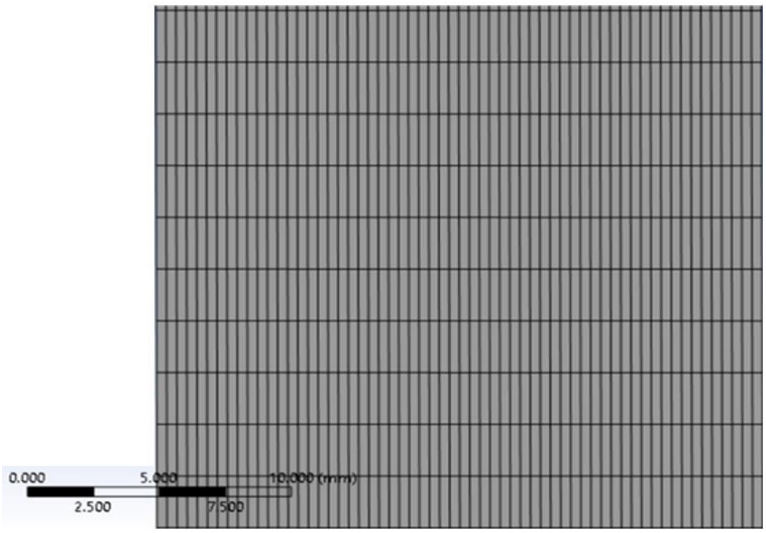

Fig. 2. A view of rectangular elements used for discretization

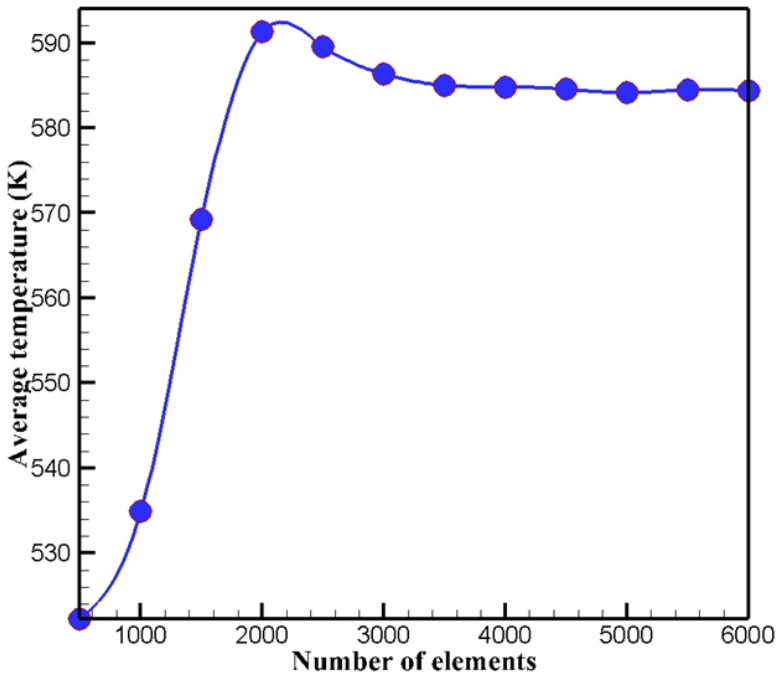

Fig. 3. Changes in the average temperature of the tank in relation to the number of elements used

Upon thorough observation of Figure 3, it is evident that as the size of the discretization components rises, the average temperature computed by the program also increases. Once the number of components reaches about 3500, the fluctuations in the computed average temperature diminish, and the graph's pattern becomes a horizontal line. This demonstrates that as the number of elements applied to the geometry hits this threshold, the generated results become unaffected by the number of elements, indicating the occurrence of solution independence from the network. Hence, the least number of components required for discretizing the geometry in this study is 3500. It is essential to acknowledge that as the number of used elements rises, the calculation speed falls, and the analysis time increases. Hence, the optimal number of elements to discretize this example is 4000. Furthermore, when considering the remaining dimensional ratios, the reduction in the area

of the geometric plane allows for determining the appropriate number of elements for computations through proportion.

3.3 Obtained Temperature Distribution Contours

Because we studied an extensive range of height-to-diameter ratios in this study, we only show the contours associated with state 3 to illustrate the generated shapes. The remaining data will be analyzed and presented in the form of graphs. In state 3, Figure 4 shows the temperature contours that show how the temperature changed over time for three different mixes of sodium nitrate with 0.5%, 1%, and 1.5% alumina. The temperature of the left, right, and upper walls has been maintained at a constant value of 600 K, while the temperature of the below-ground wall has been set at 577.95 K.

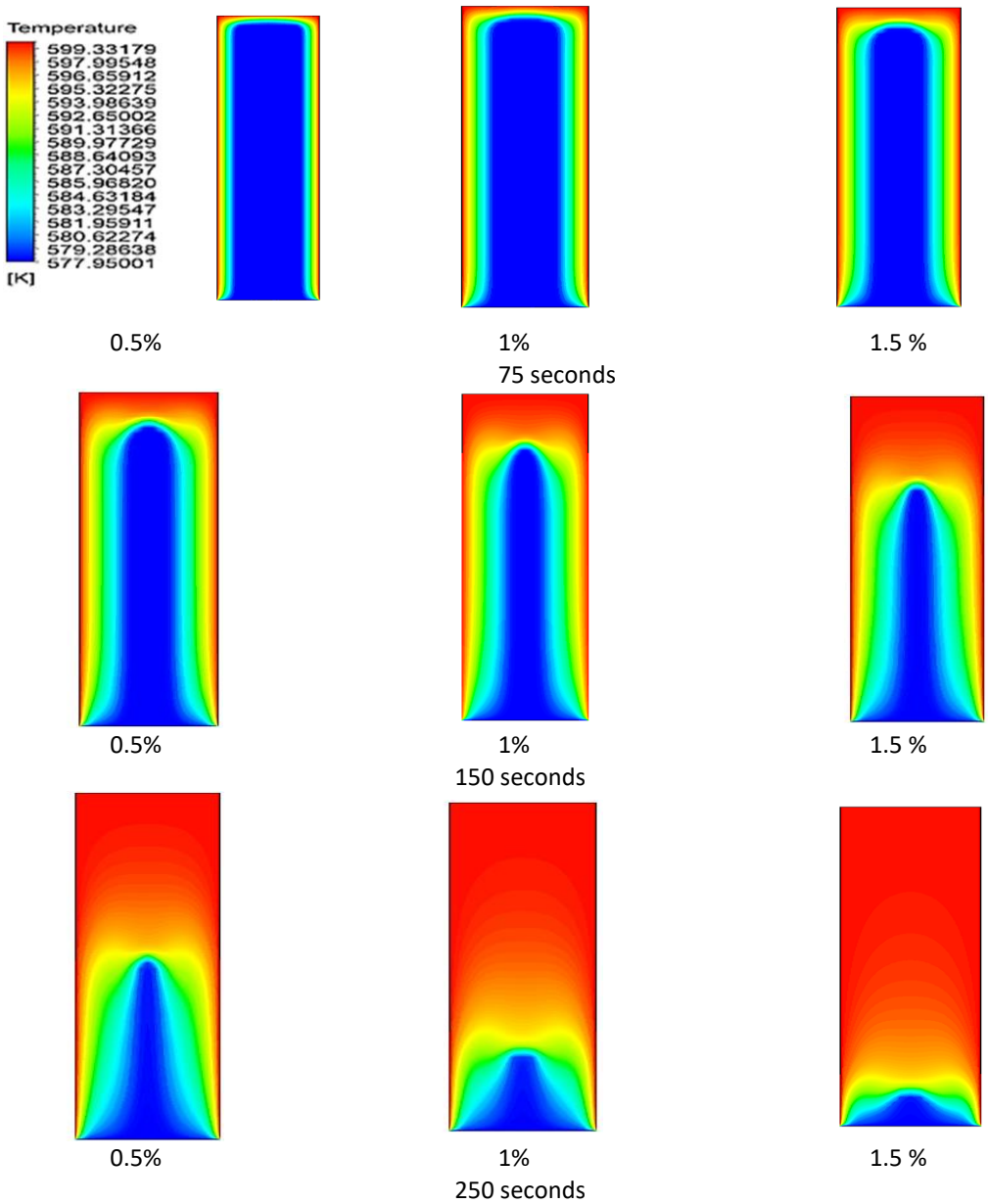

Fig. 4. Temperature distribution contour in the tank for different times and percentages of alumina in state 3

Because we studied an extensive range of height-to-diameter ratios in this study, we only show the contours associated with state 3 to illustrate the generated shapes. The remaining data will be analyzed and presented in the form of graphs. In state 3, Figure 5 shows the temperature contours that show how the temperature changed over time for three different mixes of sodium nitrate with 0.5%, 1%, and 1.5% alumina. The temperature of the left, right, and upper walls has been maintained at a constant value of 600 K, while the temperature of the below-ground wall has been set at 577.95 K.

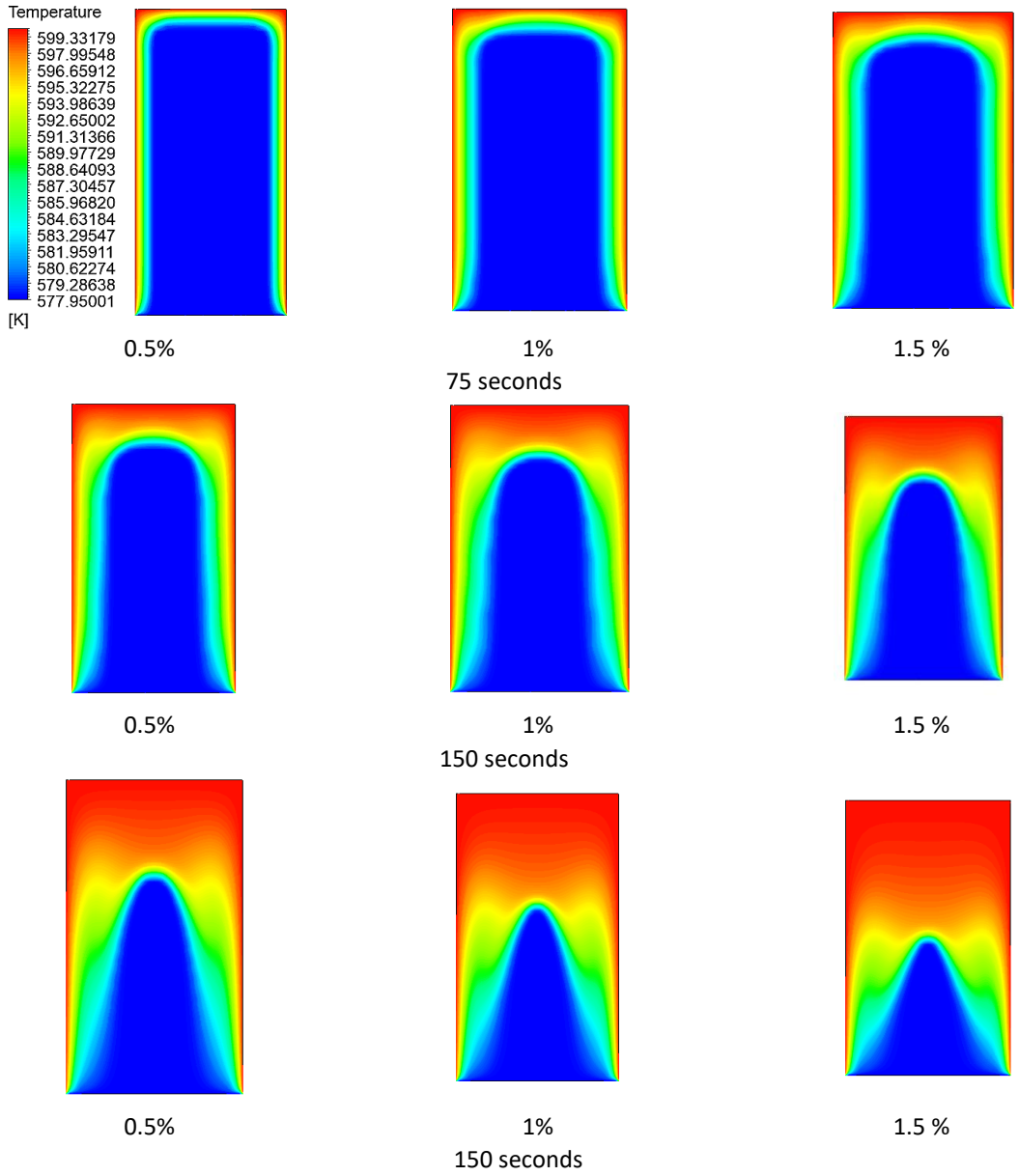

Fig. 5. Contour of temperature distribution in the tank for different times and percentages of alumina

As can be seen, the temperature distribution in the radial direction undergoes more fluctuations in this state than in State 3. Furthermore, the proportion of regions exhibiting elevated temperatures and proximity to the wall temperature diminishes compared to instance 3. The temperature contours for state nine are shown in Figure 6. This model has a width greater than its

length, making it easier to compare how the size of the tank affects the temperature distribution in the phase transition material.

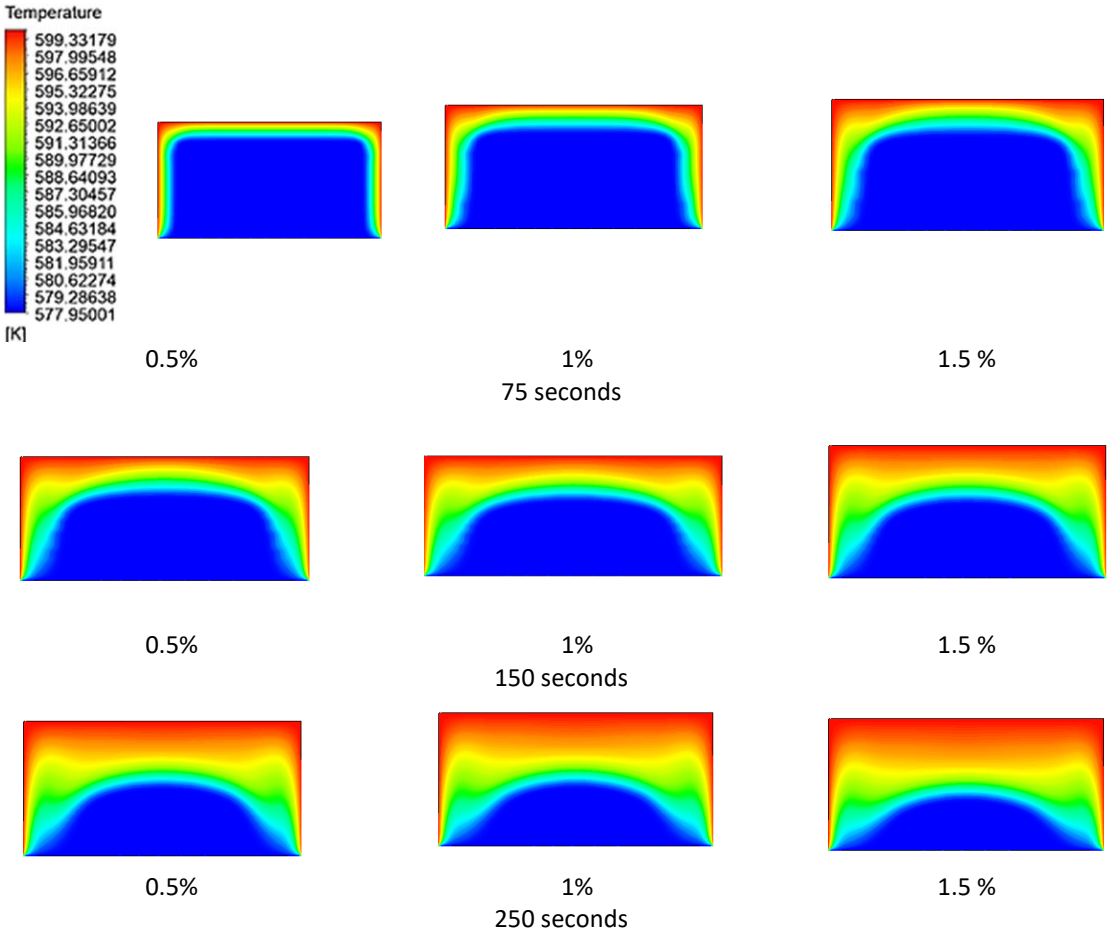

Fig. 6. Contour of temperature distribution in the tank for different times and percentages of alumina

B As seen in the image above, it is evident that increasing the ratio of the tank's diameter to its height diminishes the impact of alumina on the temperature distribution within the tank. The contour lines indicate that. The temperature distribution contour is nearly the same among the tanks containing sodium nitrate with alumina concentrations of 0.5%, 1%, and 1.5% at corresponding time intervals. When the ratio of diameter to height in tanks exceeds 1, increasing the amount of alumina in sodium nitrate does not significantly impact the temperature distribution inside the tank. Furthermore, tanks with a diameter-to-height ratio greater than 1 exhibit a volume with a minimum temperature or a temperature near the lowest temperature, compared to tanks with a height more significant than the diameter. The freezing point of the phase-changing material is higher. In other words, as the ratio of diameter to height increases, the capacity of the tank with a minimum temperature or near the freezing temperature of the phase-changing material also increases.

3.4 Liquid Volume Fraction Distribution Contours

Figure 7 illustrates a drop in the solid volume fraction within the tank over time, accompanied by a rise in melted phase transition material. Furthermore, the provided graphic illustrates that the phase change material mainly undergoes radial melting as time progresses, as indicated by the ratio

of the tank's height to its diameter. The radial melting direction of the phase-changing material occurs due to the gradual melting of the material and the subsequent increase in distance between the solid material's upper regions and the tank's upper wall, where the boundary temperature is applied. Furthermore, it is evident that with time, the molten material migrates towards the lower wall, while solid material remains in the lower wall. The specified boundary conditions for the bottom wall of the tank use the temperature required to freeze the phase transition material as the boundary temperature, which is the reason for the migration of molten material towards the lower wall while solid material remains present.

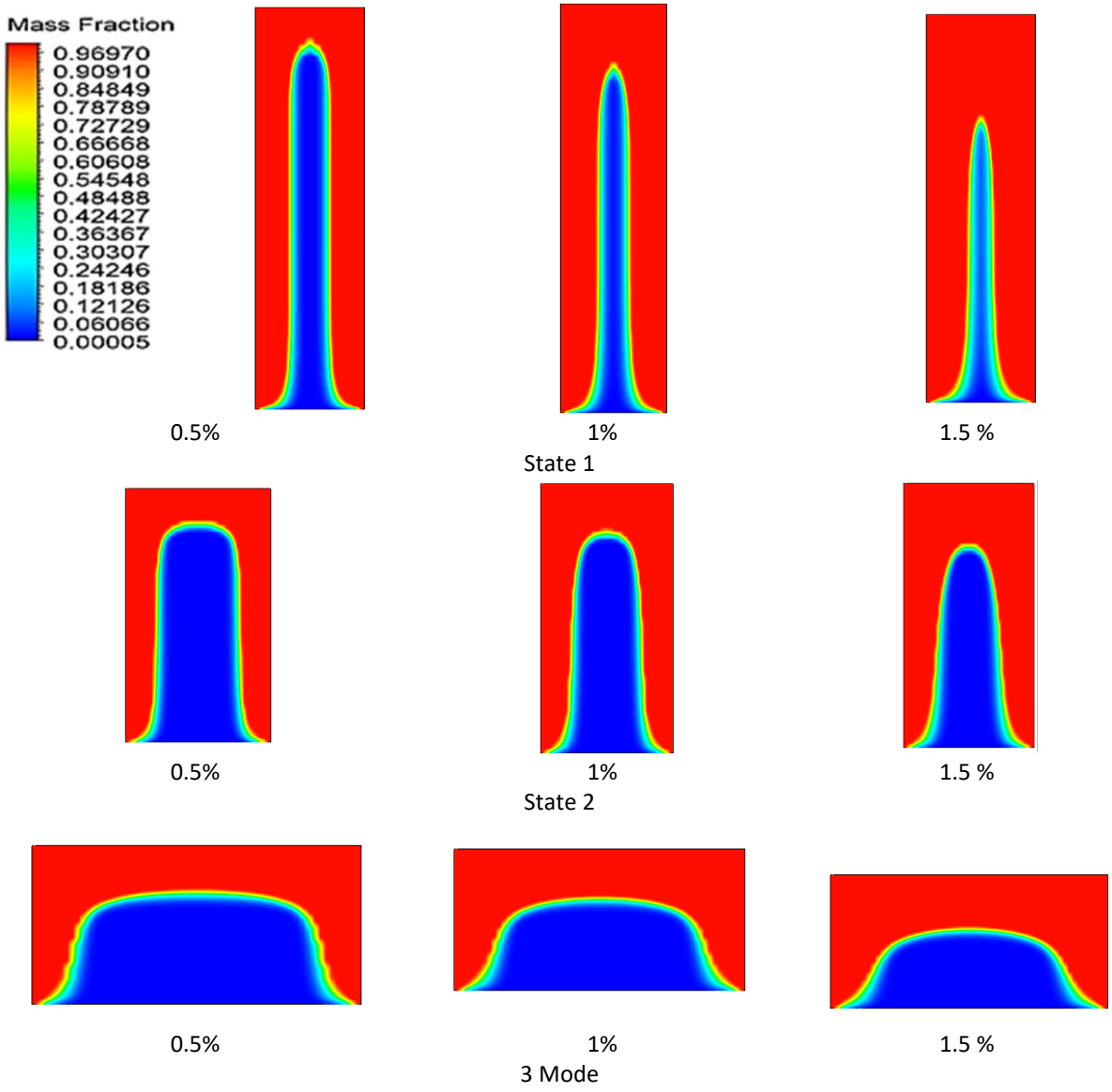

Fig. 7. Liquid fraction distribution contour in the tank for different times and percentages of alumina in 150 seconds

Decreasing the ratio of the tank's height to diameter results in a reduction in both the volume of the molten material and the effect of introducing alumina particles into sodium nitrate. Adding alumina particles to sodium nitrate has a negligible effect on its melting rate. As a result, there is a little difference in volume between the solid areas of the tank holding sodium nitrate with 0.5 percent alumina and the tank carrying sodium nitrate with 1.5 percent. The percentage of alumina cannot be detected.

3.5 Average Temperature Changes inside the Tank

The temperature fluctuations for all ten combinations of tank diameter and height in a sodium nitrate solution with 1% alumina are displayed in Figure 8. The figure illustrates the initial phase of the analysis process, where the temperature inside the tank rises rapidly due to the application of boundary conditions and the transient nature of the analysis. However, as time progresses and the phase changer reaches its melting point, the growth rate of the average temperature inside the tank slows down. This deceleration in speed continues for approximately 150 seconds. Subsequently, as the phase-change material continued to melt, the temperature rise inside the tank further escalated. This signifies a secondary phase of melting of the phase change material. Eventually, after about 250 seconds, the temperature reached its peak. The tank configuration achieves thermal equilibrium, resulting in a slower rate of temperature increase and a lowered slope on the graph.

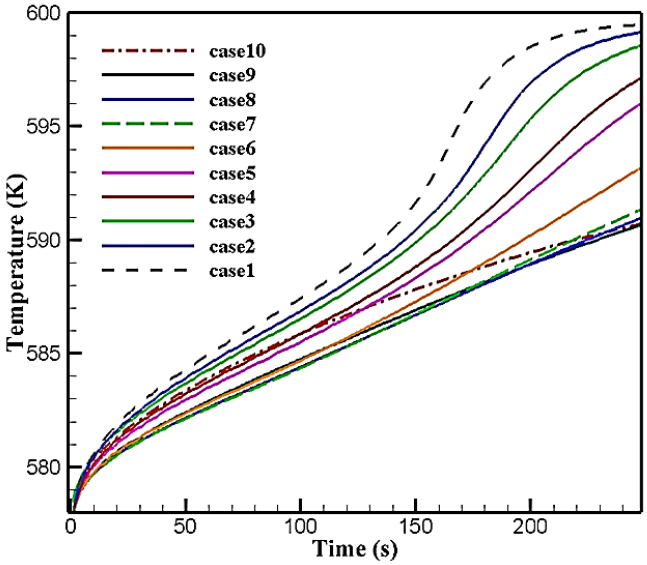

Fig. 8. Average temperature changes for all 10 states of diameter and height for the tank

In the above diagram, it is evident that when the ratio of the tank's dimensions approaches unity from state 1 to state 7 (where the tank's diameter and height are equal), the curvature of the temperature change graphs diminishes, indicating a reduction in the rate of speed changes. It functions as a phase transition catalyst during the process of melting. Furthermore, the graphs exhibit a consistent decrease in the overall slope from state 1 to state 8. However, when the ratio of the diameter to the height of the tank grows, the slope of the temperature change graphs experiences a subsequent increase. This argument suggests that the rate at which the temperature fluctuates in the tank is directly proportional to the disparity between the tank's diameter and height.

3.6 Amounts of Sodium Nitrate Dissolved Over Time

Figure 9 illustrates the variations in the proportion of liquid sodium nitrate within the tank at various time intervals. This is observed when 1% of alumina is introduced to the sodium nitrate while considering varying ratios of the tank's diameter and height. From the picture, it is evident

that when the height-to-diameter ratio is greater in the initial examples, the phase-changing material melts at a faster rate. Consequently, in the first state, the proportion of melted material volume to the total material volume within the tank is the fraction of melted material reaches nearly 1 in approximately 150 seconds in the first state. In the second state, this occurs in about 170 seconds. However, for states 7, 8, and 9, even after 250 seconds, the maximum fraction of melted material is only around 0.8. Interestingly, as the ratio of diameter to height increases, the melting speed of the material inside the tank once again deteriorates. It grows. Figure 10 illustrates the impact of alumina % on melting speed in two states: 3 and 9.

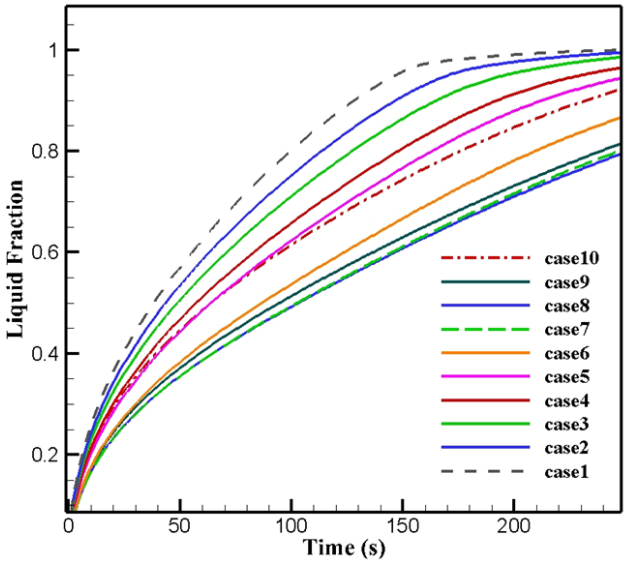

Fig. 9. Changes in the volume fraction of the molten material for different states

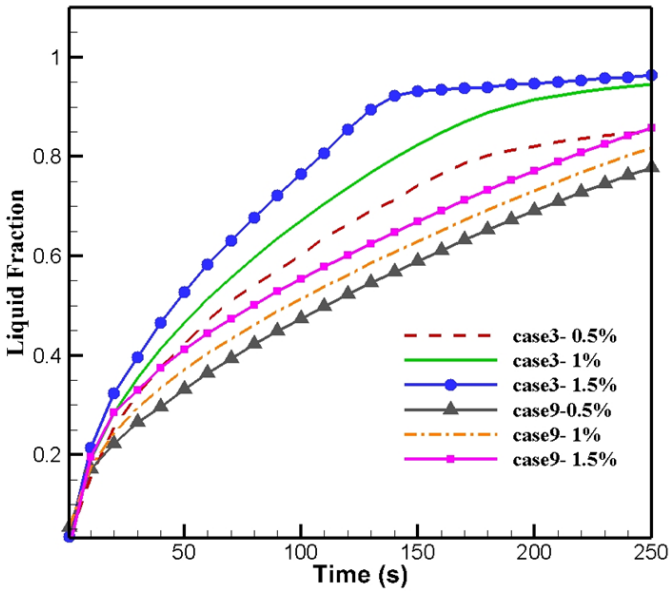

Fig. 10. Comparison of the effect of alumina percentage on melting speed in two modes 3 and 9

The liquid volume fraction distribution contour images clearly demonstrate the noticeable impact of utilising alumina particles in state 3, as seen in the above figure. As seen in the image, the melting rate of sodium nitrate in the state 3 tank rises as the proportion of alumina increases.

However, in state 9, where the ratio of the tank's height to its diameter is less than one, the addition of alumina particles to sodium nitrate has a minimal impact on the rate at which this material melts. As a result, the graphs depicting the three different concentrations of alumina in sodium nitrate for state 9 are nearly identical. The outcome was narrowly determined and shows minimal discrepancy.

4. Conclusions

The goal of this research was to use a computer program called AnsysFluent to study how well tanks store energy using materials that change from solid to liquid and back again. In this study, we looked at how the size of the tank and the amount of alumina added to the sodium nitrate affect how fast it melts and the temperature changes inside. The key findings derived from this study may be outlined as follows:

i. The rate of temperature rise in the tank is directly proportional to the amount of alumina.
ii. By augmenting the proportion of alumina included in sodium nitrate, the temperature distribution within the tank becomes more homogeneous.
iii. Increasing the alumina concentration results in more heat transfer from the tank walls to the sodium nitrate phase changer.
iv. Increasing the aspect ratio of the tank (the ratio of its diameter to its height) mitigates the impact of alumina on the temperature distribution within the tank.
v. Decreasing the tank's height-to-diameter ratio reduces the impact of adding alumina particles to sodium nitrate.
vi. Increasing the amount of alumina in sodium nitrate does not significantly impact the temperature distribution in tanks with a diameter-to-height ratio larger than 1.
vii. As the ratio of diameter to height grows, the capacity of the tank containing the phase transition material with a minimum temperature or close to freezing temperature increases.
viii. Initially, the temperature within the tank rises rapidly throughout the analysis process. However, as time progresses and the phase change material approaches its melting point, the pace at which the average temperature inside the tank climbs lowers.
ix. As the tank's dimensions transition from state 1 to state 7, where the diameter and height are identical, the temperature change graphs exhibit less curvature. This suggests a decrease in the rate at which the phase change material melts.
x. The rate of temperature change in the tank is directly proportional to the difference between the diameter and height of the tank.
xi. •In general, by reducing the ratio of the height of the tank to its diameter, the effect of adding alumina particles to sodium nitrate decreases and the storage efficiency of the source also decreases.
xii. In circumstances where the height-to-diameter ratio is bigger, the melting speed of the phase-changing material is higher. However, as the diameter-to-height ratio increases, the melting speed of the material inside the tank increases once again.

Since every scientific research should be the foundation of subsequent research and improve the process of future research, it is necessary to provide suggestions for conducting future research

at the end of each research. Among the suggestions that can be made for future research related to this research are:

i. Examining other geometries for energy storage tanks
ii. Using experimental methods to check the effectiveness of adding alumina to sodium nitrate
iii. Feasibility of using sodium nitrate as a temperature regulator in lithium batteries
iv. Checking the efficiency of other additives to phase change materials.

References

[1] Yang, Liu, Xing Jin, Yuan Zhang, and Kai Du. "Recent development on heat transfer and various applications of phase-change materials." *Journal of cleaner production* 287 (2021): 124432. https://doi.org/10.1016/j.jclepro.2020.124432
[2] Sadeghi, Hadi Mohammadjafari, Morsal Babayan, and Ali Chamkha. "Investigation of using multi-layer PCMs in the tubular heat exchanger with periodic heat transfer boundary condition." *International Journal of Heat and Mass Transfer* 147 (2020): 118970. https://doi.org/10.1016/j.ijheatmasstransfer.2019.118970
[3] Jahangiri, A., and O. Ahmadi. "Numerical investigation of enhancement in melting process of PCM by using internal fins." *Journal of Thermal Analysis and Calorimetry* 137 (2019): 2073-2080. https://doi.org/10.1007/s10973-019-08098-8
[4] Sheikholeslami, M. "Solidification of NEPCM under the effect of magnetic field in a porous thermal energy storage enclosure using CuO nanoparticles." *Journal of Molecular Liquids* 263 (2018): 303-315. https://doi.org/10.1016/j.molliq.2018.04.144
[5] Ghalambaz, Mohammad, Ali Doostanidezfuli, Hossein Zargartalebi, and Ali J. Chamkha. "MHD phase change heat transfer in an inclined enclosure: effect of a magnetic field and cavity inclination." *Numerical Heat Transfer, Part A: Applications* 71, no. 1 (2017): 91-109. https://doi.org/10.1080/10407782.2016.1244397
[6] Ghalambaz, Mohammad, Ali Doostani, Ali J. Chamkha, and Muneer A. Ismael. "Melting of nanoparticles-enhanced phase-change materials in an enclosure: effect of hybrid nanoparticles." *International Journal of Mechanical Sciences* 134 (2017): 85-97. https://doi.org/10.1016/j.ijmecsci.2017.09.045
[7] Su, Jun-Feng, Li-Xin Wang, and Li Ren. "Preparation and characterization of double-MF shell microPCMs used in building materials." *Journal of Applied Polymer Science* 97, no. 5 (2005): 1755-1762. https://doi.org/10.1002/app.21205
[8] Hawlader, M. N. A., M. S. Uddin, and H. J_ Zhu. "Preparation and evaluation of a novel solar storage material: microencapsulated paraffin." *International Journal of Solar Energy* 20, no. 4 (2000): 227-238. https://doi.org/10.1080/01425910008914357
[9] Liu, Chenzhen, Zhonghao Rao, Jiateng Zhao, Yutao Huo, and Yimin Li. "Review on nanoencapsulated phase change materials: preparation, characterization and heat transfer enhancement." *Nano Energy* 13 (2015): 814-826. https://doi.org/10.1016/j.nanoen.2015.02.016
[10] brahim B. M, Ahn H. K. Transient thermal analysis of phase change process.Transport Phenomena in Heat and Mass Transfer. 1992. https://doi.org/10.1016/B978-0-444-89851-7.50058-3
[11] Ramachandran, N., J. P. Gupta, and Y. Jaluria. "Thermal and fluid flow effects during solidification in a rectangular enclosure." *International Journal of Heat and Mass Transfer* 25, no. 2 (1982): 187-194. https://doi.org/10.1016/0017-9310(82)90004-7
[12] Shih, Yen-Ping, and Tse-Chuan Chou. "Analytical solutions for freezing a saturated liquid inside or outside spheres." *Chemical Engineering Science* 26, no. 11 (1971): 1787-1793. https://doi.org/10.1016/0009-2509(71)86023-2
[13] Velraj, R. V. S. R., R. V. Seeniraj, B. Hafner, Christian Faber, and Klemens Schwarzer. "Experimental analysis and numerical modelling of inward solidification on a finned vertical tube for a latent heat storage unit." *Solar Energy* 60, no. 5 (1997): 281-290. https://doi.org/10.1016/S0038-092X(96)00167-3
[14] Elbahjaoui, Radouane, and Hamid El Qarnia. "Performance evaluation of a solar thermal energy storage system using nanoparticle-enhanced phase change material." *international journal of hydrogen energy* 44, no. 3 (2019): 2013-2028. https://doi.org/10.1016/j.ijhydene.2018.11.116
[15] Kumar, P. Manoj, and K. Mylsamy. "A comprehensive study on thermal storage characteristics of nano-CeO2 embedded phase change material and its influence on the performance of evacuated tube solar water heater." *Renewable Energy* 162 (2020): 662-676. https://doi.org/10.1016/j.renene.2020.08.122

[16] Iachachene, Farida, Zoubida Haddad, Müslüm Arıcı, Eiyad Abu-Nada, and Mikhail A. Sheremet. "The effect of nano encapsulated phase change materials and nanoparticles on turbulent heat transport: A conical diffuser scenario." *Journal of Energy Storage* 52 (2022): 104703.

[17] Togun, Hussein, Hakim S. Sultan, Hayder I. Mohammed, Abdellatif M. Sadeq, Nirmalendu Biswas, Husam Abdulrasool Hasan, Raad Z. Homod, Adnan Hashim Abdulkadhim, Zaher Mundher Yaseen, and Pouyan Talebizadehsardari. "A critical review on phase change materials (PCM) based heat exchanger: Different hybrid techniques for the enhancement." *Journal of Energy Storage* 79 (2024): 109840. https://doi.org/10.1016/j.est.2023.109840

[18] Choure, Bhim Kumar, Tanweer Alam, and Rakesh Kumar. "A review on heat transfer enhancement techniques for PCM based thermal energy storage system." *Journal of Energy Storage* 72 (2023): 108161. https://doi.org/10.1016/j.est.2023.108161

[19] Kasper, Lukas, Dominik Pernsteiner, Alexander Schirrer, Stefan Jakubek, and René Hofmann. "Experimental characterization, parameter identification and numerical sensitivity analysis of a novel hybrid sensible/latent thermal energy storage prototype for industrial retrofit applications." *Applied Energy* 344 (2023): 121300.

[20] Righetti, Giulia, Claudio Zilio, Dario Guarda, Domenico Feo, Marco Auerbach, Martin Butters, and Simone Mancin. "Experimental analysis of a commercial size bio-based latent thermal energy storage for air conditioning." *Journal of Energy Storage* 72 (2023): 108477. https://doi.org/10.1016/j.est.2023.108477

[21] Mauricio, Carmona, Mario Palacio, and Arnold Martínez. "Experimental analysis of a flat plate solar collector with integrated latent heat thermal storage." *Contemp. Urban Aff* 1 (2017): 7-12. https://doi.org/10.25034/ijcua.2018.36zd72

[22] Bauer, Thomas, Laing Dörte, Kröner Ulrike, and Tamme Rainer. "Sodium nitrate for high temperature latent heat storage." (2009).

[23] Abbas, Ali Sabri, and Ayad Ali Mohammed. "Improvement of Plate-Fin Heat Exchanger Performance with Assistance of Various Types of Vortex Generator." *CFD Letters* 15, no. 7 (2023): 131-147. https://doi.org/10.37934/cfdl.15.7.131147

[24] Abbas, Ali Sabri, and Ayad Ali Mohammed. "Enhancement of Plate-Fin Heat Exchanger Performance with Aid of (RWP) Vortex Generator." *International Journal of Heat & Technology* 41, no. 3 (2023). https://doi.org/10.18280/ijht.410336

[25] Abbas, Ali Sabri, and Ayad Ali Mohammed. "Augmentation of Plate-Fin Heat Exchanger Performance with Support of Various Types of Fin Configurations." *Mathematical Modelling of Engineering Problems* 9, no. 5 (2022). https://doi.org/10.18280/mmep.090532

[26] Abbas, Ali Sabri, and Ayad Ali Mohammed. "Enhancement of plate-fin heat exchanger performance with aid of various types of fin configurations: a review." *Journal of Advanced Research in Fluid Mechanics and Thermal Sciences* 99, no. 2 (2022): 48-66. https://doi.org/10.37934/arfmts.99.2.4866